



HAL
open science

Microplastics in surface waters of the Gulf of Gabes, southern Mediterranean Sea: Distribution, composition and influence of hydrodynamics

Amal Zayen, Sami Sayadi, Cristele Chevalier, Moncef Boukthir, Sana Ben Ismail, Marc Tedetti

► To cite this version:

Amal Zayen, Sami Sayadi, Cristele Chevalier, Moncef Boukthir, Sana Ben Ismail, et al.. Microplastics in surface waters of the Gulf of Gabes, southern Mediterranean Sea: Distribution, composition and influence of hydrodynamics. *Estuarine, Coastal and Shelf Science*, 2020, 242, pp.106832. 10.1016/j.ecss.2020.106832 . hal-02658422

HAL Id: hal-02658422

<https://hal.science/hal-02658422>

Submitted on 14 Apr 2023

HAL is a multi-disciplinary open access archive for the deposit and dissemination of scientific research documents, whether they are published or not. The documents may come from teaching and research institutions in France or abroad, or from public or private research centers.

L'archive ouverte pluridisciplinaire **HAL**, est destinée au dépôt et à la diffusion de documents scientifiques de niveau recherche, publiés ou non, émanant des établissements d'enseignement et de recherche français ou étrangers, des laboratoires publics ou privés.



Distributed under a Creative Commons Attribution - NonCommercial 4.0 International License

Microplastics in surface waters of the Gulf of Gabes, southern Mediterranean Sea: Distribution, composition and influence of hydrodynamics

Amal Zayen^{a,*}, Sami Sayadi^{b,**}, Cristele Chevalier^c, Moncef Boukthir^d,
Sana Ben Ismail^e, Marc Tedetti^{a,c}

^aLaboratoire des Bioprocédés Environnementaux, Centre de Biotechnologie de Sfax, BP 1177, 3018, Sfax, Tunisia

^bCenter for Sustainable Development, College of Arts and Sciences, Qatar University, 2713, Doha, Qatar

^cAix Marseille Université, Université de Toulon, CNRS, IRD, MIO UM 110, 13288, Marseille, France

^dLaboratoire des Matériaux et Fluides, Institut Préparatoire aux Etudes d'Ingénieur de Tunis, University of Tunis, 2 Boulevard Lel Nehru, 1089 Montfleury, Tunisia

^eLaboratoire Milieu Marin, Institut National des Sciences et Technologies de la Mer, Tunisia

The Mediterranean Sea has been described as one of the most affected areas by marine litter in the world. Although microplastics and their effects have been investigated in this area, most of the currently available studies have been limited to the northwestern part of the basin. This study constitutes a first attempt to determine the abundance, characteristics and composition of microplastics in near surface waters of the Gulf of Gabes (southern Mediterranean Sea, Tunisia). Samples were collected using a 200 μm -mesh size trawl net along two transects. The study revealed an average concentration of 63,739 items/ km^2 where fragments and films were the most frequent microplastics. Polyethylene, reformulated polyethylene and polypropylene were the most abundant plastics identified among the samples (86–100%). The influence of hydrodynamics on microplastics in the Gulf of Gabes was investigated through the use of a Lagrangian tracking model to simulate the dispersion of particles in water. Modelling results seem to be in agreement with the reported distribution and characteristics of microplastics in this area.

1. Introduction

Because of their unique properties, plastic materials are used in a wide range of application sectors and in our daily lives. As a result, plastic yearly production has exceeded the 340 million tons mark (PlasticsEurope, 2018). Although it exists a great variety of types, applications and life cycles for plastics, most of them are designed for a short service time or single use applications, such as plastic bags, with low value recovery and difficulty to degrade (Wang et al., 2016). The sharp contrast between the remarkable durability of plastic materials and their short service time has led to the accumulation of plastic wastes in the environment. Plastics have been reported in the ocean, in lakes, in rivers and even in aquatic and terrestrial animals due to ingestion (Dümichen et al., 2017). In particular, marine plastic litter is estimated to increase by one order of magnitude by 2025 when considering the

level of expected future demand and discharges of plastics (Jambeck et al., 2015). When plastics debris undergo environmental impacts like sunlight, oxidizing atmosphere and mechanical stress, polymer degradation occurs, yielding small polymer particles (Dümichen et al., 2017).

Microplastics (MPs), according to the National Oceanic and Atmospheric Administration (NOAA), are plastic particles smaller than 5 mm in size (Masura et al., 2015). MPs have either been intentionally manufactured to be small (primary MPs) or have fragmented from larger plastic items (secondary MPs) (UNEP, 2016). MP pollution in the marine environment is the cause of several hazardous and ecologically damaging effects. Owing to their small size, these particles are considered bioavailable to organisms throughout the food web (Galloway et al., 2017). In the accumulation zones, their concentrations are in the same range than zooplankton concentrations, thus increasing the risk of ingestion by zooplankton predators (Collignon et al., 2012). In addition,

* Corresponding author.

** Corresponding author.

E-mail addresses: amal.zayen@gmail.com (A. Zayen), sami.sayadi@gmail.com (S. Sayadi).

toxic chemicals, such as bisphenol A, polycyclic aromatic hydrocarbons, pesticides and polychlorinated biphenyls have been frequently found in oceanic plastic debris (Hirai et al., 2011). These substances, added to plastics during production or adsorbed from the environment, are an environmental concern since they extend the degradation times of plastic and may, in addition, leach out, introducing potentially hazardous chemicals to the biota (Cole et al., 2011).

The first reports on MPs in surface waters already date back to the early 1970s (Carpenter and Smith, 1972). At that time, these reports have got little public impact. According to the results of 24 expeditions (2007–2013) across all five sub-tropical gyres, coastal Australia, Bay of Bengal and the Mediterranean Sea, almost 270,000 tons of plastic would be currently floating in the oceans giving an estimation of a minimum of 5.25 trillion particles weighting 268,940 tons (Avio et al., 2017).

The Mediterranean Sea is a semi-enclosed basin subjected to anthropogenic disturbances, especially along the coasts, and has been recently proposed as one of the most impacted regions of the world with regards to MPs (Cózar et al., 2015; Faure et al., 2015; Pedrotti et al., 2016; Suaria et al., 2016). In recent years, many studies have been undertaken to assess and better understand MP pollution in this area. High amounts of plastic debris have been reported on the seafloor (Pham et al., 2014) and surface waters of Mediterranean Sea (Collignon et al., 2012; Suaria and Aliani, 2014; Ruiz-Orejón et al., 2016, 2018; Suaria et al., 2016; Van der Hal et al., 2017; Schmidt et al., 2018).

Hydrodynamic conditions such as driving forces, winds and currents influence the transport of MPs as well as their abundance, distribution and weathering processes (Veerasingam et al., 2016). MP transportation modelling should therefore be dependent upon necessary assumptions, as well as the quality of hydrodynamic forcing data. Combined hydrodynamic-Lagrangian transportation models, with different degrees of realism, have been recently proposed to forecast the transport and distribution of floating debris in the Mediterranean Sea (Lebreton et al., 2012; Eriksen et al., 2014; Mansui et al., 2015; Ourmier et al., 2018). Most of the currently available studies on the abundance of floating micro-sized particles, either based on sampling/observations or numerical simulations have, however, been limited to the northwestern part of the Mediterranean basin.

The Gulf of Gabes (GG), located in the south-east of Tunisia, is identified as one of the eleven consensus eco-regions within the Mediterranean Sea according to its physical, biogeochemical and biological characteristics (Ayata et al., 2018). This shallow and phytoplankton bloom area is strongly influenced by hydrodynamics, mainly driven by tides and anticyclonic winds (see review by Béjaoui et al., 2019). Despite the importance of the GG at the Mediterranean Basin level, to our knowledge, no data about MPs in surface waters are currently available in this region.

In this context, the objectives of the present study are 1) to investigate, for the first time, the distribution and the physico-chemical characteristics of MPs in surface waters of the GG, and 2) to assess the potential influence of hydrodynamics on the MP distribution through the use of a Lagrangian tracking model to simulate the dispersion of MP particles in water. In a lesser extent, the potential impact of biological activity is also examined. By providing the first data about MPs in surface waters of the GG, it is expected that this study will contribute to MP management in this area.

2. Materials and methods

2.1. Study area

The GG, located in the south-east of Tunisia in the southern Mediterranean Sea, is known for its high productivity and biodiversity (Ayata et al., 2018; Béjaoui et al., 2019). However, due to the rapid urbanization and industrialization of the shoreline, particularly in the northern (Sfax city) and central parts (Gabes city) of the GG, the quality of the marine environment has been deteriorating gradually (Darmoul, 1988;

Ayadi et al., 2014; Rabaoui et al., 2015; El Zrelli et al., 2017). In Gabes city area, many untreated industrial and domestic wastewaters are continuously discharged in the open sea from the industrial complex of Ghannouch-Gabes and the local municipal wastewater treatment plant, respectively (El Zrelli et al., 2018). While issues such as the degradation of the ecological environment, red tides, and eutrophication have received increasing attention, no data are available about MP pollution in surface waters in this area.

The GG is characterized by a wide continental shelf, where the bathymetry is shallower than 30 m for large stretches away from the coast. Beneath its shallow waters, the GG bottoms are composed of extensive sections of gently sloping continental shelves. Isobaths 50 m deep are reached 110 km offshore, the isobath 70 m is nearly 140 km away from the coastline, while depths of 200 m are not reached until 400 km from the coast (Fig. 1).

2.2. Microplastic sampling and *in situ* measurements

MP sampling was conducted during the MERITE cruise from 30 October to November 3, 2017 onboard the vessel “*Rahma*”, in the central part of the GG, off Ghannouch-Gabes industrial complex. Floating MP samples were collected at 8 stations (Fig. 1) using a trawl net (0.6 m in width \times 0.2 m in height) mounted with a 200- μ m mesh size. A flowmeter equipment (HYDRO-BIOS) was fixed in the middle of the trawl frame. The net was deployed from the side of the vessel and towed horizontally under low swell conditions, at an average speed of 3.5 knots for 30–45 min for each sampling transect. The flowmeter allowed for the determination of the accurate covered distance, as well as the filtered seawater volume, based on the covered distance and the trawl frame surface. Starting GPS coordinates, covered distance, surface area and filtered volume for each station are provided in Table 1. The net was then lifted out and rinsed thoroughly from the outside using seawater to concentrate all adhered particles into the cod-end. Collected samples were sieved through a 200- μ m mesh size stainless steel sieve and transferred to 500-mL glass bottles and fixed with 70% ethanol. All samples were stored at 4 °C until laboratory analyses.

Besides MP collection, *in situ* measurements of temperature and salinity were performed with a 19plus conductivity temperature depth (CTD) profiler (SeaBird Electronics Inc., SBE19plusV2 SN 6573).

2.3. Treatment and analysis of microplastic samples

In the laboratory, MP samples retained on the 200- μ m mesh size sieve were separated using steel tweezers and transferred to a glass beaker using minimal rinsing with ultrapure (Milli-Q) water. Wet peroxide oxidation procedure was conducted to remove the remaining organic matter in the sample according to Zhang et al. (2017). Twenty mL of aqueous 0.05 M Fe (II) solution (prepared by adding 7.5 g of FeSO₄·7H₂O to 500 mL of water and 3 mL of concentrated sulfuric acid) and 30% H₂O₂ solution were added to the beaker containing the 0.2-mm size fraction of collected solids. The mixture was then heated on a 75 °C hotplate for 30 min. The reaction was repeated until no natural organic material is visible. Solids in the mixed solution were filtered through a glass fiber filter (GF/F Whatman, 47-mm diameter, 0.7- μ m pore size) using a vacuum filtration system. Subsequently, the filter was placed in clean Petri dish which was covered with tinfoil paper and allowed to dry for further analysis.

Filters were analyzed under a stereomicroscope (Olympus BX 51) to sort and measure MPs with a diameter less than 4 mm, while a ruler was used to record the diameter of MPs with a greater diameter. Images of MPs were taken with a camera attached to the stereomicroscope (Olympus DP 70). Only particles with a diameter less than 5 mm were taken into account while pieces with a greater diameter were excluded from any further analysis.

The chemical composition of 463 plastic items was identified by Fourier Transform Infrared Spectroscopy (FT-IR) spectra, using a FTIR

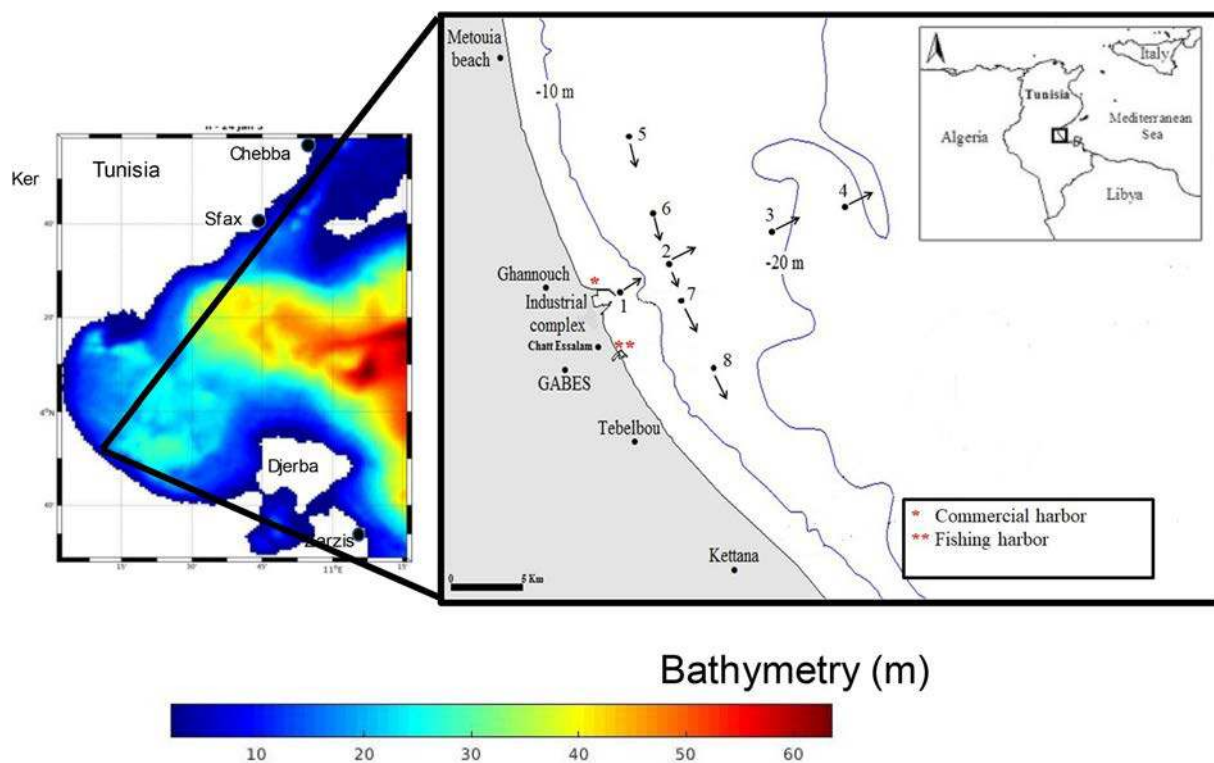


Fig. 1. Map of the study area in the Gulf of Gabes (southern Mediterranean Sea, Tunisia). Dots and arrows indicate the position of stations and the directions of the trawling net, respectively.

Table 1
Sampling information, and number and abundance of microplastics collected.

Station	Starting coordinates		Covered distance (m)	Covered surface area (m ²)	Filtered volume (m ³)	Number of items	Abundance (items km ⁻²)
1	33° 55.595' N	10° 07.063' E	3062.4	1837.4	367.5	134	72,928
2	33° 56.733' N	10° 08.876' E	4083.9	2450.3	490.1	274	111,821
3	33° 58.840' N	10° 12.666' E	4523.1	2713.9	542.8	178	65,589
4	33° 59.930' N	10° 15.500' E	6473.4	3884.0	776.8	362	93,202
5	34° 01.767' N	10° 06.295' E	4776.6	2866.0	573.2	73	25,471
6	33° 58.840' N	10° 07.623' E	5429.4	3257.6	651.5	137	42,055
7	33° 56.100' N	10° 09.240' E	3571.5	2142.9	428.6	86	40,133
8	33° 54.277' N	10° 10.400' E	3917.4	2350.4	470.1	138	58,712

spectrometer (Nicolet iS50 FT-IR) using Attenuated Total Reflectance (ATR) mode with 8 cm⁻¹ resolution and 16 scans. All spectra were recorded in the absorbance mode in the 4000–600 cm⁻¹ region. The contact between the analyzed sample and the diamond of the ATR accessory was ensured by screwing a clamp device. Plastic items identified by FTIR were randomly selected.

2.4. Contamination prevention

To avoid contamination, several precautions were taken at each step of MPs sampling, treatment and analysis. Only metal and glass equipment was used. Samples were stored in glass containers, thoroughly cleaned prior to use. During samples processing, cotton lab coats were worn and the laboratory area was maintained clean. Air circulation was kept to a minimum in order to avoid air-borne particles. Exposure of samples to air was minimum and limited to transfer between containers, which were kept covered during the rest of the time. Given the fact that contamination during MPs sampling and processing consisted only of the “fibers” coding group of MP litter, and no other groups of litter were noted (Güven et al., 2017), any fibers suspected of being of a textile origin were excluded from the analysis. According to Cózar et al. (2015), potential textile fibers can be detected thanks to their shape and

rigidness, ranging from hundreds of microns to centimeters in length and from one to few tens of microns in width. Finally, the stereomicroscope and FTIR spectrometer were cleaned and inspected carefully before use to prevent fiber contamination.

2.5. Hydrodynamics and microplastic transport modelling

The hydrodynamic model used in this study is based on the Regional Oceanic Modelling System (ROMS, Haidvogel et al., 2008; <http://mroms.org>), a three-dimensional primitive equation, and finite difference hydrodynamic model. ROMS solves the primitive equations in an earth-centered rotating environment. It is nonlinear with Boussinesq and hydrostatic approximations and uses a terrain-following, σ coordinates. The interaction of surface gravity waves and currents is considered. The model area extends along 700 km of the Tunisian coast, from Ras Kaboudia in the north (32.5°N) to the Tunisian-Libyan border in the south (35.5°N) and from 10°E to 12.5°E (Fig. 1). The horizontal grid resolution was chosen to be 1/96° (nearly 1 km) for a better representation of the small-scale processes. Grid spacing in sigma coordinates was used in the vertical with 25 levels. The bathymetry is deduced from the Tunisian Ministry of Equipment database (MEHAT) in shallow bathymetry (Othmani et al., 2017) and from Smith and

Sandwell topography (Smith and Sandwell, 1997) database in deeper bathymetry by a bilinear interpolation of the depth data. At the continental boundaries, the bathymetry is set to 1 m. The daily mean values of temperature, salinity, total velocity and elevation were transferred from the coarse spaced grid of MED12 (Lebeaupin Brossier et al., 2013) to the finely spaced grid of the ROMS open boundaries through an off-line, one-way asynchronous nesting. In the framework of this study, the model was forced by all the forcing likely to contribute to the hydrodynamics of the GG. The meteorological forcing used is from the European Centre for Medium Range Weather Forecast (ECMWF), available from <http://www.ecmwf.int>, based on 6-hourly records has been applied. It involves ERA-Interim project (1979–2018). The effects of tides were taken into account. The model was initialized with the temperature and salinity fields provided by the MEDATLAS monthly climatology (MEDAR/MEDATLAS Group, 2002). The daily mean values of temperature, salinity, total velocity and elevation were transferred from the coarse spaced grid of MED12 (Lebeaupin Brossier et al., 2013) to the finely spaced grid of the ROMS open boundaries through an off-line, one-way asynchronous nesting.

To understand the role of hydrodynamics in the distribution of MPs at the different stations, a 3D Lagrangian tracking model (ICHTHYOP; Lett et al., 2008) was implemented to simulate the dispersion of MP particles due to 3D currents. Ichthyop is a free Java tool designed to study the effects of physical and biological factors on the ichthyoplankton dynamics. The same numerical approach has been successfully applied to study the circulation and accumulation of floating litter in the Mediterranean Sea (Macias et al., 2019) and in identifying distribution and accumulation patterns of floating marine debris in the Black Sea (Miladinova et al., 2020).

The transport is calculated thanks to the movement equation reduced to the horizontal advection which is constraint by the velocity field previously obtained with the hydrodynamic ROMS model. Hence the MP trajectories depend on the tide, on the wind effect on the water velocity, on mesoscale current and also on water column thermohaline structure but the Stokes drift induced by the wave effect is neglected. Indeed, according to some previous studies (Kubota, 1994; Martinez et al., 2009; Miladinova et al., 2020), the major role in marine debris accumulation is played by surface currents. Moreover, Kubota (1994) found that Stokes drift does not significantly contribute to debris transport. A buoyancy force due to the difference between the particle and surrounding water density was considered. Then, MPs were considered as passive surface tracers. Under these hypothesis, a set of backward simulations where 1000 particles were advected backward in time was performed for three months recording the GPS position of each particle every day. The departure was set at the surface in each station and the studied area is the one described by the hydrodynamics model. The aim is to determine where water sampled came from and which route it followed.

2.6. Statistical analysis

Box-and-whisker plots, Mann-Whitney non-parametric tests (U test), Spearman principal component analysis (PCA) and hierarchical ascendant classification (HAC) applied on selected MP parameters were performed using XLSTAT 2013.5.01 (Microsoft Excel add-in program). HAC was used in order to find homogenous groups of individuals (stations) within the dataset, with respect to selected variables. These groups (or clusters) present a low within-variability and are different than others (displaying high between-variability). The dissimilarity measurement between clusters was based on Ward's method, which uses squared Euclidean distance. Variable values were centered and reduced beforehand. The threshold of significance was set at $p < 0.05$. Colour maps of CTD data were carried out using Ocean Data View (ODV) software version 4.6.5 (Schlitzer, R., <http://odv.awi.de>, 2014). The spatial interpolation/gridding of data was conducted using Data-Interpolating Variational Analysis (DIVA) (Barth et al., 2010; Troupin et al., 2012).

3. Results

3.1. Description of Gulf of Gabes circulation

It is worth noting that the tidal range of the GG is the most important of the whole Mediterranean Sea (up to 2 m in height) as reported by previous studies (Tsimplis et al., 1995; Abdennadher and Boukthir, 2006; Sammari et al., 2006). Hence, the circulation is influenced by the tide, by the wind and by the mesoscale current flowing along the Tunisian continental shelf, namely the Atlantic Tunisian Current (ATC) a permanent surface current with an Atlantic origin (Sorgente et al., 2003; Boukthir et al., 2019).

One ATC branch invades the GG, particularly in winter, and recirculates anticyclonally, whereas the second branch continues flowing southeastward as an important coastal current and becomes close to the Libyan coast, giving rise to a strong coastal jet near the Libyan current (Supporting Fig. 1a and b), which was identified as the Atlantic Libyan Current (ALC) (Sorgente et al., 2011; Ben Ismail et al., 2015). Our model results are in agreement with the scheme of surface circulation of modified Atlantic water based on the altimetry data that has been proposed by Jebri et al. (2016). Another important result of our model is the current reversals between winter and summer along the south-east coast of the GG (Supporting Fig. 1a and b). This result is in agreement with the trajectories of the drifting buoys 1 and 2 (Supporting Fig. 1c and d) launched respectively in November 2017 and July 2018 (Sammari and Chevalier, personal communication). Indeed, in November the buoy moved south-eastward, while in July it moved north-westward.

Fig. 2 shows the hydrodynamic circulation under neap-tidal forcing 10 days before MP sampling. The hydrodynamic circulation in the GG region was controlled by the tide, wind and current at boundaries. Instantaneously, the circulation oscillated under tidal forcing. During the flood, the current was oriented towards the coast whereas during the ebb, it was off-ward. During slack water, eddies may appear, namely during neap tide. During low water, counter-clock wise eddies appeared along the coast, near Gabes, and a clockwise eddy in the middle of the gulf. In contrast, during high water, counter-clock wise eddies were present in the middle of the gulf, and clockwise eddies near Boughrara lagoon and Kerkennah Island. These eddies decreased at spring tide in front of the intense tidal current (Fig. 2).

A tidally-averaged coastal current was observed flowing from the north to the south, probably in link with wind and the regional current (Fig. 3). However, eddies disturbed this littoral current, namely the two great eddies in the middle of the gulf, which may induce a counter littoral current from Djerba to Gabes (Fig. 3).

3.2. Temperature and salinity

The spatial distribution of temperature and salinity in the surface waters of the GG is displayed in Fig. 4. Temperature ranged from 21.75 to 23.5 °C (Fig. 4a), and salinity from 39.2 to 39.5 (Fig. 4b). The littoral current from north to south with colder and less salty water is clearly visible on stations 1, 2, 5, 6, 7 and 8, whereas the station 3 seems to be marked by a recirculate water, warmer (23.5 °C) and saltier (39.5). Water at station 4 seems to follow the littoral current, but more offshore with temperature and salinity around 22.75 °C and 39.3, respectively (Fig. 4a and b).

3.3. Microplastic abundance and distribution

MPs were found at all stations, with an item number ranging from 73 MP particles (station 5) to 362 MP particles (station 4) (Supporting Table 1). The total number of MPs collected was 1382 MP particles (Table 1). To determine the MP abundance (in items/km²), the number of MP was divided by the sampling surface area (in km²). The latter was calculated by multiplying the net width by the covered (sampling) distance, derived from the flowmeter data. The MP abundance varied

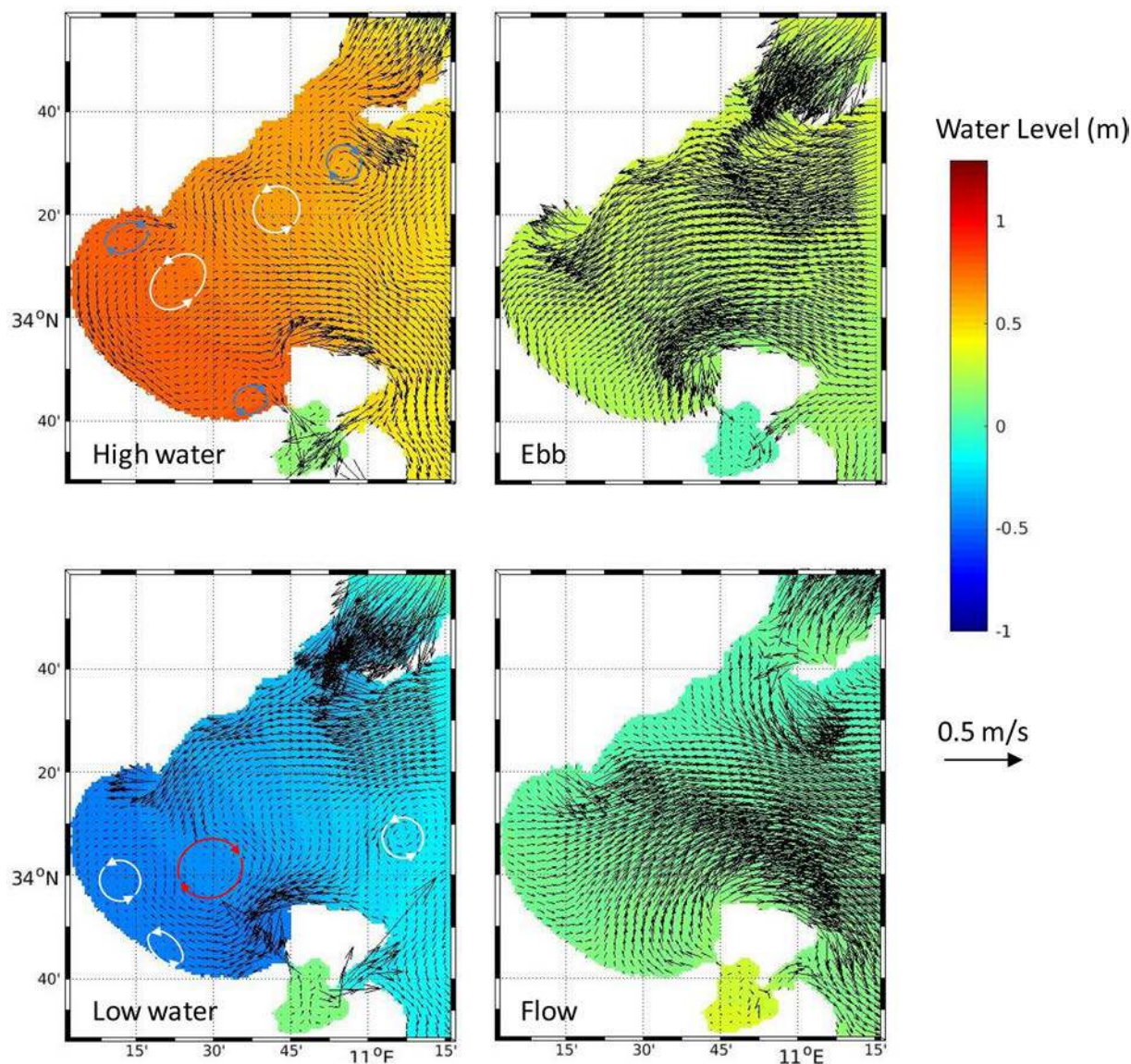


Fig. 2. Hydrodynamic circulation under neap-tidal forcing 10 days before microplastic sampling.

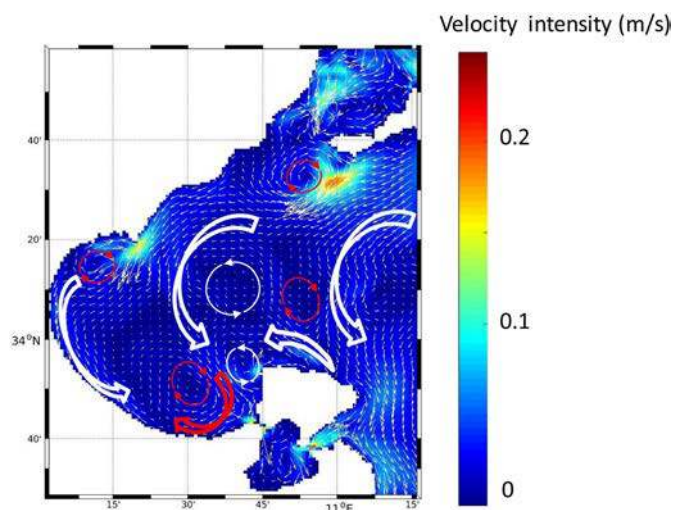


Fig. 3. Example of tidally averaged hydrodynamic circulation at the sampling day and modeled temperature during the numerical experiment.

between 25,471 items/km² (station 5) and 111,821 items/km² (station 2) (Table 1) with a mean value of 63,739 items/km². This range was quite high considering the relatively limited study area. Station 4, located 24 km off the coast (Fig. 1), showed a high MP abundance with 93,202 items/km².

3.4. Characteristics of microplastics

Collected MPs were categorized based on their shapes, colours, size class and polymer types. Fig. 5 shows examples of collected MPs with different shapes, colours and sizes.

3.4.1. Shape

Collected MPs were sorted into five different categories: fragments, films, filaments, pellets and foam (Fig. 6a and b). Pellets and foam were combined in accordance with their low abundance. Fragments dominated, with on average $34,692 \pm 16,756$ items/km², accounting for 58 \pm 19% of the total number of MPs for the eight stations (Fig. 6a). Fragments varied from approximately 30% close to the harbour (station 1) to more than 80% in the most northern station (station 5) (Fig. 6b). Films were also abundant, with a mean of $24,796 \pm 21,988$ items/km²

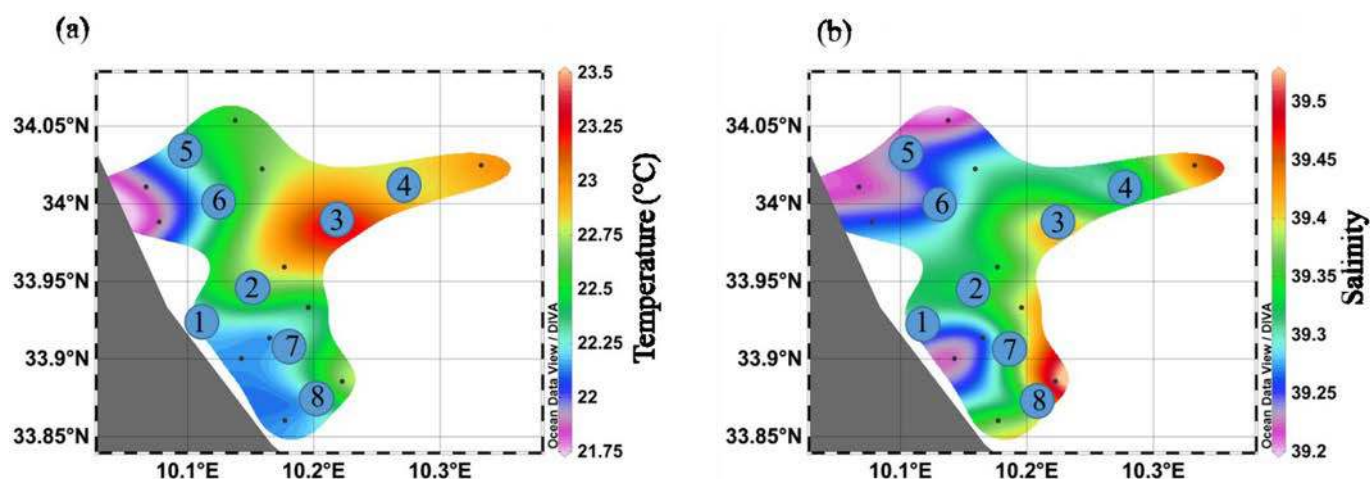


Fig. 4. Distribution of temperature (°C) (a) and salinity (b) in surface waters of the Gulf of Gabes. Blue dots indicate microplastic sampling stations while black dots indicate MERITE stations (where temperature and salinity have been actually measured). Spatial interpolation was made using Data-Interpolating Variational Analysis (DIVA) method from Ocean Data View (ODV) software version 4.6.5, Schlitzer, R., <http://odv.awi.de>, 2014. (For interpretation of the references to colour in this figure legend, the reader is referred to the Web version of this article.)

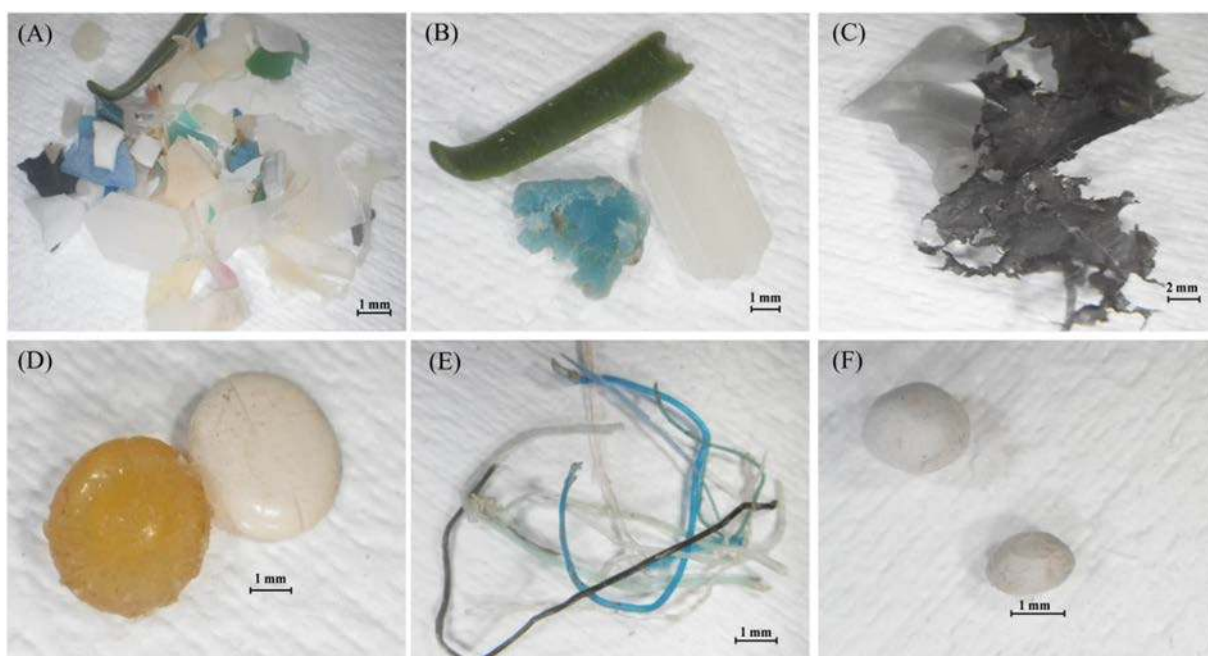


Fig. 5. Examples of microplastics with different shapes, colours and sizes: general view (a), fragments (b), films (c), pellets (d), filaments (e), and polystyrene balls (f). (For interpretation of the references to colour in this figure legend, the reader is referred to the Web version of this article.)

($34 \pm 18\%$ of total MPs) for all stations (Fig. 6a). This mean film abundance was not significantly different from that of fragments (*U* test, $p = 0.130$). Films represented from 12% (station 5) to 62% (station 2) of total MPs (Fig. 6b). Filaments were found in all samples but with a relatively lower proportion ($7 \pm 4\%$ on average for all stations) (Fig. 6a and b). Foams and pellets accounted together for 1% on average of total MPs. Foams were present in stations 1, 3 and 8, whereas pellets were exclusively detected in stations 1 and 4 (Fig. 6a and b). With regard to the abundance of fragments and films, station 4 and station 2 appeared respectively as outliers, with significantly higher values compared to the other stations (Fig. 6a).

3.4.2. Colour

The colour of MPs may increase their bioavailability owing to prey items resemblance (Wright et al., 2013). In this study, most of MP items

were white (for all stations, mean abundance of $26,272 \pm 15,245$ items/ km^2 , $74 \pm 12\%$ of total items), while blue, black, green and red items accounted on average for 9, 5, 5 and 3% of total MPs, respectively (Fig. 6c and d). Other colours including, yellow, orange, grey and purple were also present within MPs (4% of total MPs). According to the abundance of white MPs, station 4 was an outlier, with significantly higher values compared to the other stations (Fig. 6c).

3.4.3. Size class

Collected MP size ranged from 0.2 to 5 mm. Items were thus categorized into three classes: 0.2–1, 1–2 and 2–5 mm (Fig. 6e and f). The mean abundance and percentage of small-sized MPs (0.2–1 mm), medium-sized MPs (1–2 mm) and large-sized MPs (2–5 mm) were $10,682 \pm 7038$ items/ km^2 and $36 \pm 26\%$, $12,786 \pm 5903$ items/ km^2 and $38 \pm 15\%$, and $11,224 \pm 14,591$ items/ km^2 and $26 \pm 22\%$, respectively.

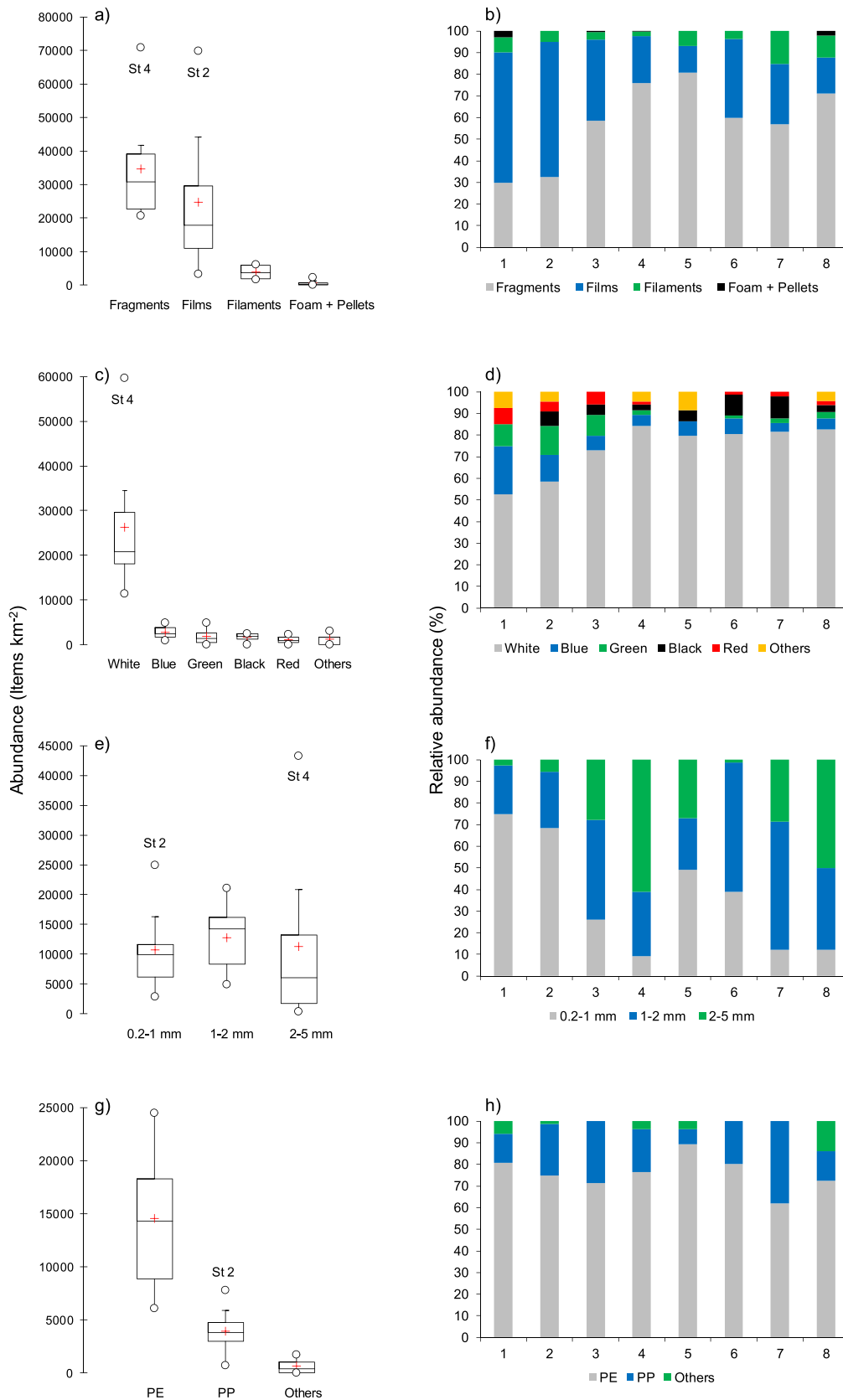


Fig. 6. Box-and-whisker plots of microplastic abundance (items/km²), and their relative abundance (%) for each station with regard to shapes (a, b), colours (c, d), size classes (e, f) and polymer types (g, h). The bottom and top of the box plot are the 25th and 75th percentiles, respectively, whereas the central line is the 50th percentile (the median), and the red cross is the mean. The ends of the error bars correspond to the 10th percentile (bottom) and to 90th percentile (top). Dots are the minimal and maximal values. Dots located above the error bar are considered as outliers, i.e., station 2 and/or station 4. (For interpretation of the references to colour in this figure legend, the reader is referred to the Web version of this article.)

The mean abundances for the three size classes were not significantly different (U test, $p = 0.328\text{--}0.645$). As shown in Fig. 6f, the relative contributions of the size classes varied significantly according to the sampling station. The 0.2–1 mm size class accounted for over 65% of the total recovered MPs close to the coast (stations 1 and 2), but for less than 10% in station 4 (offshore station). The 1–2 mm size class represented between 46 and 60% of the total MPs in stations 3, 6 and 7. The 2–5 mm size class was dominant for station 4 (61%), and in a lesser extent, station 8 (50%), but represented only 1–6% of total MPs in stations 1, 2 and 6 (Fig. 6f). Regarding the abundance of 0.2–1 mm and 2–5 mm MP, station 2 and station 4 appeared respectively as outliers, with significantly higher values compared to the other stations (Fig. 6e).

3.4.4. Polymer type

The MP chemical composition may also provide relevant information on the origin of individual items (Galgani et al., 2015). In all collected samples, the overwhelming majority of items subjected to FT-IR analysis were attributed to polyolefins, basically polyethylene and reformulated polyethylene (PE) with $14,545 \pm 6661$ items/km² and $76 \pm 8\%$ of total MPs for all stations (Fig. 6g and h). Polypropylene (PP) particles were also present in samples with 3918 ± 2219 items/km² and $21 \pm 10\%$ of total MPs. Other polymers accounted for 3% of total MPs (Fig. 6g and h). The polymer composition was much more homogenous between stations than was the size class. Ethylene-propylene copolymer, a class of synthetic rubber produced by copolymerizing ethylene and propylene and frequently used in packaging and manufacturing carrier bags, was also detected. The overwhelming majority of recovered filaments were also attributed to PE and may be derived from ropes and fishing nets.

3.4.5. Multivariate analyses

Fig. 7 shows Spearman PCA applied on the main MP parameters for the eight stations, i.e., abundance (items/km²) of fragments, films, white particles, 0.2–1, 1–2 and 2–5 mm size MPs, as well as PE particles. Correlation circle (on the left) displayed significant positive (linear) correlations between abundances of fragments, white and 1–2 mm size MPs ($r = 0.88\text{--}0.98$, $n = 8$, $p < 0.05$), between abundances of films and PE MPs ($r = 0.91$, $n = 8$, $p < 0.05$), and between abundances of white and 2–5 mm size MPs ($r = 0.74$, $n = 8$, $p < 0.05$).

The first principal component (PC1), which explained 53.7% of total variability within samples, was mainly driven by abundances of fragments, white, 1–2 mm and 2–5 mm size MPs (Fig. 7). PC1 allowed the

discrimination between three groups of stations: i) stations 1, 2, 5–7, ii) stations 3, 8, and iii) station 4, with increasing abundances of fragments, white, 1–2 mm and 2–5 mm size MPs. The second principal component (PC2) accounted for 35.8% of total variability within samples, and was mostly correlated to abundances of films and PE MPs (Fig. 7). PC2 allowed separating three groups of stations: i) stations 5, 7, 8, ii) stations 3, 4, 6, and iii) stations 1, 2, with increasing abundances of films and PE MPs. Overall, according to PC1 and PC2, three groups of stations were highlighted (blue circles): i) stations 1, 2, ii) stations 3, 5–8, and iii) station 4. These three groups were also confirmed by the hierarchical ascendant classification applied on the same dataset (figure not shown). Consequently, multivariate analyses highlighted the offshore station 4 as particular sample with the highest abundances of fragments, white, 1–2 mm and 2–5 mm size MPs.

4. Discussion

4.1. Features of microplastics in the Gulf of Gabès

As no standardized MP sampling method has been established so far, methodological differences (type of sampling net, mesh size and extraction method) limit comparisons of MP abundances with previous results. A comparison of our MP abundances with those acquired in the Mediterranean Sea with similar sampling methods and measurement units revealed that MP abundances we recorded in the GG region were, in many cases, one order of magnitude lower than those found in other Mediterranean areas (Table 2). Some potential non-permanent aggregation zones of marine debris in the Mediterranean Sea were numerically identified namely the Gulf of Sirte, as well as the northwestern Mediterranean and the Tyrrhenian sub-basins. These possible retention areas are either the result of weak dynamics or the rotating behaviour of the general surface circulation in this area (Mansui et al., 2015). Many studies based merely on sampling campaigns (i.e., not numerical simulations) have confirmed the presence of numerous plastic debris in these areas (Ruiz-Orejón et al., 2016; Pedrotti et al., 2016; Suaria et al., 2016) (Table 2).

Although MP abundance in the GG was overall lower compared to other Mediterranean areas, a quite significant spatial variability appeared, with a higher abundance offshore (station 4) relative to the coast (Figs. 6 and 7). This observation is in line with the findings of Pedrotti et al. (2016), who noted that stations located at long distances

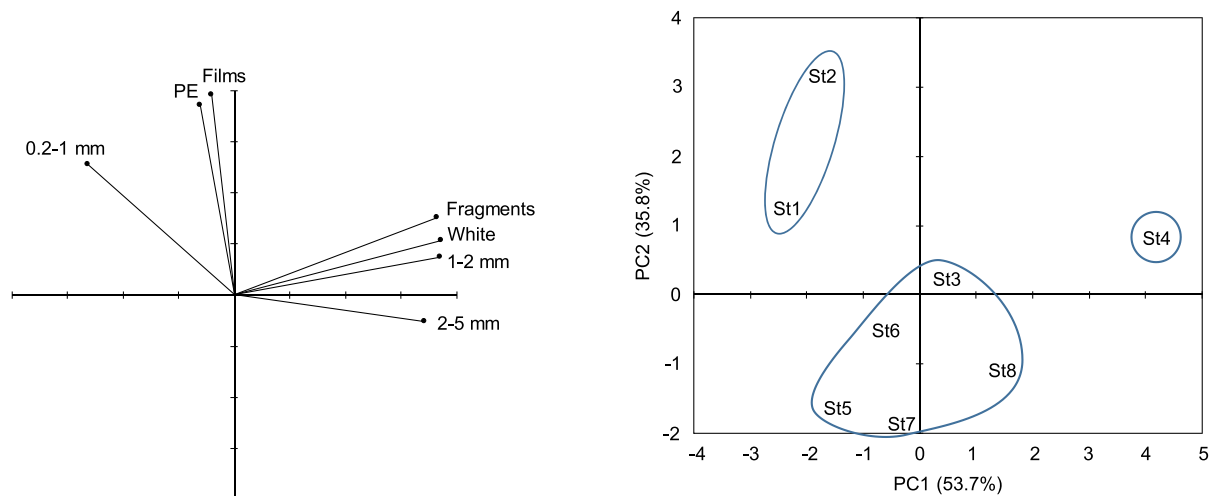


Fig. 7. Principal component analysis (PCA), based on the Spearman's correlation matrix, applied on selected microplastic parameters, i.e., abundance (items/km²) of fragments, films, white particles, 0.2–1, 1–2 and 2–5 mm size microplastics, polyethylene and reformulated polyethylene (PE) microplastics. Projection of variables (left) and samples (right) on the first factorial plane (PC1 versus PC2). Three groups of samples are highlighted from this PCA (blue circles) and confirmed by the hierarchical ascendant classification: group 1 = stations 1 and 2, group 2 = stations 3, 5–8, and group 3 = station 4. (For interpretation of the references to colour in this figure legend, the reader is referred to the Web version of this article.)

Table 2

Comparison of abundance of microplastics in the surface waters of the Gulf of Gabès (present study) with those reported in other Mediterranean areas.

Location	Net mesh	Abundance (items/km ²)	Reference
Central and Western Mediterranean Sea	333 μ m	8999–1,164,403	Ruiz-Orejón et al. (2016)
Ligurian Sea (northwestern Mediterranean Sea)	330 μ m	21,000–578,000	Pedrotti et al. (2016)
Central-western Mediterranean Sea	200 μ m	40,000–9,230,000	Suaria et al. (2016)
Mediterranean coast of Turkey	330 μ m	16,339–520,213	Güven et al. (2017)
Northern Ionian Sea (Greece)	–	0 – 1,610,000	Digka et al. (2018)
Gulf of Lion (northwestern Mediterranean Sea),	780 μ m 330 μ m	6000–1,000,000	Schmidt et al. (2018)
Gulf of Gabes (Tunisia)	200 μ m	25,471–111,821	This study

from land, far from the influence of perimetric currents, showed the highest MP abundances. This has also been frequently reported in offshore areas of low dispersion and surface convergence, identified as accumulation regions for the floating plastics (Eriksen et al., 2014; Cózar et al., 2015).

Our results highlight the dominance of fragments, and, in a lesser extent, films within MPs (Fig. 6a and b), which is in agreement with several other works (Ruiz-Orejón et al., 2016; Tunçer et al., 2018). The predominance of fragments over other collected items suggests that the source of MPs is rather related to the breakdown of larger plastic products (secondary sources) than to MP primary inputs, such as MP directly released from treated wastewater effluents. As many previous studies (see review by Hidalgo-Ruz et al., 2012), most of the identified items were of white colour (Fig. 6c and d). Colour can be also considered as a good indicator of MP residence time in the ocean and their weathering degree (Pan et al., 2019). Almost all collected MP items during our field survey showed fading hues, indicating they underwent various aging processes over a long period of time.

The patterns of MP size distribution can be related to their origin and might also reflect their degree of weathering. It was suggested that plastic aging process and weather forcing help to break large marine plastic debris into smaller pieces, resulting in a decrease in the size of MPs (Pan et al., 2019). This study revealed high dominance of the smaller MP items close to the coast (stations 1 and 2) (Fig. 6e and f; Fig. 7), which may indicate a rapid fragmentation along the shoreline. The fact that large-sized items were in the majority offshore (station 4) may suggest that MPs in this area were of different origin relative to MPs collected closer to the coast (Fig. 6e and f; Fig. 7) (see below the link with hydrodynamics).

PE and PP are the most frequently recorded polymers in all environmental compartments in the Mediterranean Sea (Pedrotti et al., 2016; Digka et al., 2018) consonantly with their large manufacture and use worldwide. Frequent detection of these polymers can be also related to their low density, making them buoyant and easily transported in surface marine waters. Other polymers, such as polyamide resin and polyether urethane, were also observed. Here, only polystyrene balls were identified as polystyrene, and were mainly present at station 1, located a few kilometres from the harbour, suggesting that their probable source is containers for seafood packaging (Fig. 6g and h; Fig. 7). It is noteworthy to mention that other polymers such as polyethylene terephthalate (PET) and polyvinyl chloride (PVC), frequently reported in many previous studies (Suaria et al., 2016; Digka et al., 2018) were not detected in our studied area (Fig. 6g and h).

Therefore, some features are highlighted in the GG concerning MPs: 1) lower abundances and a lower diversity of polymer types (strong dominance of PE and PP) compared to other Mediterranean regions, and

2) an atypical offshore site (station 4) that exhibits different MP characteristics (higher abundances, higher sizes) relative to other stations (Fig. 7). Below we argue about the potential influence of hydrodynamics and biological activity on these observed features.

4.2. Potential influence of hydrodynamics and biological activity

The potential influence of hydrodynamics on the distribution and characteristics of MPs in the GG region was analyzed using the Lagrangian Ichtyop model. In simulations, we observe that the water that was present at each station has come from outside of the Gulf (Fig. 8). It entered in the Gulf through the north few months before (2–3 months) the sampling date and has probably travelled to sampling stations thanks the littoral currents. The main part of sampled water has remained near the coast, passing near coastal cities, such as Sfax. Only water sampled in station 4 was mainly coming farther from the coast behind the Kerkennah Island. Some part of water sampled in stations 8 and 3 may have a quite similar origin to that of station 4 (Fig. 8). The results indicate that MPs in station 4 were carried by a different water mass and could be considered as more representative of MPs of the Mediterranean Sea basin. This can better explain the atypical nature of this station compared to other sites in terms of abundance, shapes, colours and sizes, as described above. From the MP characteristics described here, it seems that particles collected at all other stations (stations 1, 3–8) were less aged and less altered than those of station 4. These less aged MPs could originate from cities located on the coastal area of the GG, such as Sfax city. The latter, which is the second-largest city and one of the main industrial-port centre in Tunisia, may be a significant source of MPs to marine waters through inputs from various wadis and effluents, as well as atmospheric deposition (Fourati et al., 2018). Sfax is located in the northern part of the GG, in front of the Kerkennah Islands. Hence, MPs issued from Sfax would be transported to stations 1, 3–8 through north-south littoral currents (Fig. 8). In contrast, according to modelling results, MPs at station 4 would come from far more distant areas, possibly outside the GG, carried by different water masses.

Another feature revealed during this study was the relatively low MP abundance and polymer diversity in the GG region. This may be attributed to an exacerbated sinking of buoyant MPs due to the intrinsic nature of particles (i.e., their polymer composition, which influences their density) but also to local meteorological conditions and environmental factors (Kowalski et al., 2016). Among these factors, biofouling

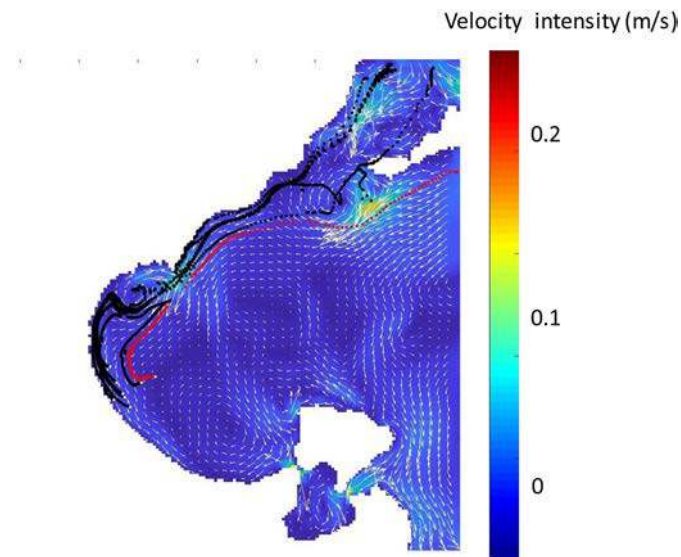


Fig. 8. Three-months median trajectory before the microplastic sampling day. Black plots indicate the trajectory of sampled water at stations 1, 2, 3, 5, 6, 7 and 8, whereas red plots indicate the trajectory of sampled water at station 4.

process (colonization of MPs by the marine biota) could have a significant role in the MP sinking and their subsequent “depletion” in surface waters. Indeed, GG has been characterized as a bloom region with a strong phytoplankton biomass induced by high nutrients concentrations through terrestrial (atmospheric) or sediments inputs (Ayata et al., 2018; Béjaoui et al., 2019). During this work, the presence of biofouled MP items was frequently observed during sample processing. Consequently, besides hydrodynamics, particle sinking induced by biofouling process might also influence the distribution of MPs in surface waters of the GG.

5. Conclusions

This study revealed an average MP concentration of 63,739 items/km² in the Gulf of Gabes. This oceanic area, which is considered as one of the eleven “consensus” eco-regions within the Mediterranean Sea (Ayata et al., 2018) appears particular with respect to its microplastic content. Indeed, this mean concentration is quite low compared to those reported in other Mediterranean regions. Also, MPs in the Gulf of Gabes are characterized by the dominance of fragments and films, as well as polyethylene materials. Interestingly, a high heterogeneity was observed for the MP distribution on a small spatial scale (samples taken at few kilometers from each other). This may be attributed to several factors including the hydrodynamic conditions and biofouling. We show through Lagrangian modelling that MPs in offshore station 4 were very likely carried by a different water mass and could be considered as more representative of MPs of the Mediterranean Sea basin. This can better explain the atypical nature of this station compared to other sites. This work thus emphasizes the pertinence of the coupling modelling/observations for the study of the MP distribution. As a result, future spatio-temporal studies are needed in order to gain a better understanding of the MP dynamics in this region.

Declaration of competing interest

The authors declare no competing interests.

Acknowledgements

We acknowledge the Tunisian Ministry of Higher Education and Scientific Research for providing a post-doctoral scholarship for Dr. A. Zayen. This work was financially supported by the CNRS,INSU MIS-TRALS MERMEX-MERITE project and the IRD French-Tunisian International Joint Laboratory (LMI) “COSYS-Med”. We acknowledge the “Institut National des Sciences et Technologies de la Mer” (INSTM) for their logistic support, as well as the captain and the crew of the vessel “*Rhama*” for their technical help during the cruise. We warmly thank C. Sammari (INSTM) for the cruise organisation and management, H. Taba (INSTM) and M. Pagano (MIO/INSTM) for providing the microplastic net, as well as S. Mounier (MIO) and J.M. Robert (MAPIEM-SIM) for the use of the FTIR instrument. We are grateful to two anonymous Reviewers for their very helpful and relevant comments on this manuscript.

References

Abdennadher, J., Boukthir, M., 2006. Numerical simulation of the barotropic tides in the Tunisian shelf and the strait of Sicily. *J. Mar. Syst.* 63, 162–182.
 Avio, C.G., Gorbi, S., Regoli, F., 2017. Plastics and microplastics in the oceans: from emerging pollutants to emerged threat. *Mar. Environ. Res.* 128, 2–11. <https://doi.org/10.1016/j.marenvres.2016.05.012>.

Ayadi, N., Aloulou, F., Bouzid, J., 2014. Assessment of contaminated sediment by phosphate fertilizer industrial waste using pollution indices and statistical techniques in the Gulf of Gabes (Tunisia). *Arab. J. Geosci.* 8, 1755–1767.
 Ayata, S.D., Irissou, J.O., Aubert, A., Berline, L., Dutay, J.C., Mayot, N., Nieblas, A.E., D’Ortenzio, F., Palmieri, J., Reygondeau, G., Rossi, V., Guieu, C., 2018. Regionalisation of the Mediterranean basin, a MERMEX synthesis. *Prog. Oceanogr.* 163, 7–20.
 Barth, A., Alvera Azcarate, A., Troupin, C., Ouberdous, M., Beckers, J.-M., 2010. A web interface for gridding arbitrarily distributed in situ data based on Data-Interpolating Variational Analysis (DIVA). *Adv. Geosci.* 28, 29–37.
 Béjaoui, B., Ben Ismail, S., Othmani, A., Ben Abdallah-Ben Hadj Hamida, O., Chevalier, C., et al., 2019. Synthesis review of the Gulf of Gabes (eastern Mediterranean Sea, Tunisia): morphological, climatic, physical oceanographic, biogeochemical and fisheries features. *Estuar. Coast Shelf Sci.* 219, 395–408.
 Ben Ismail, S., Sammari, C., Béranger, K., 2015. Surface Circulation Features along the Tunisian Coast: Central Mediterranean Sea. 26th IUGG General Assembly. Prague, Czech Republic, June 22 – July 2th.
 Boukthir, M., Ben Jaber, I., Chevalier, C., Abdennadher, J., 2019. A high-resolution three-dimensional hydrodynamic model of the gulf of Gabes (Tunisia). In: 42nd CIESM Congress.
 Carpenter, E.J., Smith Jr., K.L., 1972. Plastics on the sargasso sea surface. *Science* 175, 1240–1241.
 Cole, M., Lindeque, P., Halsband, C., Galloway, T.S., 2011. Microplastics as contaminants in the marine environment: a review. *Mar. Pollut. Bull.* 62, 2588–2597.
 Collignon, A., Hecq, J.H., Galgani, F., Voisin, P., Collard, F., Goffart, A., 2012. Neustonic microplastic and zooplankton in the north western Mediterranean Sea. *Mar. Pollut. Bull.* 64, 861–864.
 Cózar, A., Sanz-Martín, M., Martí, E., González-Gordillo, J.I., Ubeda, B., Gálvez, J.Á., Irigoien, X., Duarte, C.M., 2015. Plastic accumulation in the Mediterranean Sea. *PLoS One* 10, 1–12.
 Darmoul, B., 1988. Pollution dans le Golfe de Gabès (Tunisie): bilan des six années de surveillance (1976–1981). *Bulletin de l’Institut National des Sciences et Technologies de la Mer de Salammbô* 15, 61–84.
 Digka, N., Tsangaris, C., Kaberi, H., Adamopoulou, A., Zeri, C., 2018. Microplastic abundance and polymer types in a mediterranean environment. In: *Proceedings of the International Conference on Microplastic Pollution in the Mediterranean Sea*. Springer Water. Springer, Cham, pp. 17–24.
 Dümichen, E., Eisentraut, P., Bannick, C.G., Barthel, A.K., Senz, R., Braun, U., 2017. Fast identification of microplastics in complex environmental samples by a thermal degradation method. *Chemosphere* 174, 572–584.
 El Zrelli, R., Courjault-Radé, P., Rabaoui, L., Daghouj, N., Mansour, L., Balti, R., Castet, S., Attia, F., Michel, S., Bejaoui, N., 2017. Biomonitoring of coastal pollution in the Gulf of Gabes (SE, Tunisia): use of *Posidonia oceanica* seagrass as a bioindicator and its mat as an archive of coastal metallic contamination. *Environ. Sci. Pollut. Control Ser.* 24, 22214–22225.
 El Zrelli, R., Rabaoui, L., Ben Alaya, M., Daghouj, N., Castet, S., Besson, P., Michel, S., Bejaoui, N., Courjault-Radé, P., 2018. Seawater quality assessment and identification of pollution sources along the central coastal area of Gabes Gulf (SE Tunisia): evidence of industrial impact and implications for marine environment protection. *Mar. Pollut. Bull.* 127, 445–452.
 Eriksen, M., Lebreton, L.C.M., Carson, H.S., Thiel, M., Moore, C.J., Borrero, J.C., et al., 2014. Plastic pollution in the world’s oceans: more than 5 trillion plastic pieces weighing over 250,000 tons afloat at sea. *PLoS One* 9 (12), e111913, 10.1371/journal.pone.0111913 PMID: 25494041.
 Faure, F., Saini, C., Potter, G., Galgani, F., De Alencastro, L.F., Hagmann, P., 2015. An evaluation of surface micro- and mesoplankton pollution in pelagic ecosystems of the Western Mediterranean Sea. *Environ. Sci. Pollut. Control Ser.* 22, 12190–12197.
 Fourati, R., Tedetti, M., Guigue, C., Goutx, M., Garcia, N., Zaghden, H., Sayadi, S., Elleuch, B., 2018. Sources and spatial distribution of dissolved aliphatic and polycyclic aromatic hydrocarbons in surface coastal waters from the Gulf of Gabès (Tunisia, Southern Mediterranean Sea). *Prog. Oceanogr.* 163, 232–247.
 Galgani, F., Hanke, G., Maes, T., 2015. Global distribution, composition and abundance of marine litter. In: Bergmann, M., Gutow, L., Klages, M. (Eds.), *Marine Anthropogenic Litter*. Springer, Berlin, pp. 29–56.
 Galloway, T.S., Cole, M., Lewis, C., 2017. Interactions of microplastic debris throughout the marine ecosystem. *Nat. Ecol. Evol.* 1, 116.
 Güven, O., Gökdağ, K., Jovanović, B., Kideys, A.E., 2017. Microplastic litter composition of the Turkish territorial waters of the Mediterranean Sea, and its occurrence in the gastrointestinal tract of fish. *Environ. Pollut.* 223, 286–294.
 Haidvogel, D.B., Arango, H., Budgell, W.P., Cornuelle, B.D., Curchitser, E., et al., 2008. Ocean forecasting in terrain-following coordinates: formulation and skill assessment of the Regional Ocean Modeling System. *J. Comput. Phys.* 227, 3595–3624.
 Hidalgo-Ruz, V., Gutow, L., Thompson, R.C., Thiel, M., 2012. Microplastics in the marine environment: a review of the methods used for identification and quantification. *Environ. Sci. Technol.* 46, 3060–3075.
 Hirai, H., Takada, H., Ogata, Y., Yamashita, R., Mizukawa, K., Saha, M., Kwan, C., Moore, C., Gray, H., Laursen, D., Zettler, E.R., Farrington, J.W., Reddy, C.M., Peacock, E.E., Ward, M.W., 2011. Organic micropollutants in marine plastics debris from the open ocean and remote and urban beaches. *Mar. Pollut. Bull.* 62, 1683–1692.
 Jambeck, J.R., Geyer, R., Wilcox, C., Siegler, T.R., Perryman, M., Andrady, A., Narayan, R., Law, K.L., 2015. Plastic waste inputs from land into the ocean. *Mar. Pollut. Bull.* 347, 768–771.
 Jebri, F., Birol, F., Zakardjian, B., Bouffard, J., Sammari, C., 2016. Exploiting coastal altimetry to improve the surface circulation scheme over the central Mediterranean Sea. *J. Geophys. Res. Ocean.* 121, 4888–4909.

- Kowalski, N., Reichardt, A.M., Waniek, J.J., 2016. Sinking rates of microplastics and potential implications of their alteration by physical, biological, and chemical factors. *Mar. Pollut. Bull.* 109, 310–319.
- Kubota, M., 1994. A mechanism for the accumulation of floating marine debris north of Hawaii. *J. Phys. Oceanogr.* 24, 1059–1064.
- Lebeau-pin Brossier, C., Drobinkki, P., Béranger, K., Bastin, S., Orain, F., 2013. Ocean memory effect on the dynamics of coastal heavy precipitation preceded by a mistral event in the northwestern Mediterranean. *Q. J. R. Meteorol. Soc.* 139, 1583–1597.
- Lebreton, L.C.M., Greer, S.D., Borrero, J.C., 2012. Numerical modelling of floating debris in the world's oceans. *Mar. Pollut. Bull.* 64, 653–661.
- Lett, C., Verley, P., Mullon, C., Parada, C., Brochier, T., Penven, P., Blanke, B., 2008. A Lagrangian tool for modelling ichthyoplankton dynamics. *Environ. Model. Software* 23, 1210–1214.
- Macías, D., Cózar, A., García-Gorriz, E., Gonzalez, D., Stips, A., 2019. Surface water circulation develops seasonally changing patterns of floating litter accumulation in the Mediterranean Sea. A modelling approach. *Mar. Pollut. Bull.* 149, 110619. <https://doi.org/10.1016/j.marpollbul.2019.110619>.**
- Mansui, J., Molcard, A., Ourmières, Y., 2015. Modelling the transport and accumulation of floating marine debris in the Mediterranean basin. *Mar. Pollut. Bull.* 91, 249–257.
- Martinez, E., Maamaatuaiahutapu, K., Taillandier, V., 2009. Floating marine debris surface drift: convergence and accumulation toward the South Pacific subtropical gyre. *Mar. Pollut. Bull.* 58, 1347–1355.
- Masura, J., Baker, J., Foster, G., Arthur, C., 2015. Laboratory Methods for the Analysis of Microplastics in the Marine Environment: Recommendations for Quantifying Synthetic Particles in Waters and Sediments. NOAA Technical Memorandum NOS-OR&R-48.
- MEDAR/MEDATLAS Group, 2002. MEDAR/MEDATLAS 2002 Database. Cruise Inventory, Observed and Analysed Data of Temperature and Bio-Chemical Parameters (4 CD-ROMs).
- Miladinova, S., Macías, D., Stips, A., García-Gorriz, E., 2020. Identifying distribution and accumulation patterns of floating marine debris in the Black Sea. *Mar. Pollut. Bull.* 153, 110964.
- Othmani, A., Béjaoui, B., Chevalier, C., Elhmaidi, D., Devenon, J.L., Aleya, L., 2017. High-resolution numerical modelling of the barotropic tides in the Gulf of Gabes, eastern Mediterranean Sea (Tunisia). *J. Afr. Earth Sci.* 129, 224–232.
- Ourmières, Y., Mansui, J., Molcard, A., Galgani, F., Poitou, I., 2018. The boundary current role on the transport and stranding of floating marine litter: the French Riviera case. *Contin. Shelf Res.* 155, 11–20.
- Pan, Z., Guo, H., Chen, H., Wang, S., Sun, X., Zou, Q., Zhang, Y., Lin, H., Cai, S., Huang, J., 2019. Microplastics in the northwestern Pacific: abundance, distribution, and characteristics. *Sci. Total Environ.* 650, 1913–1922.
- Pedrotti, M., Petit, S., Eléneau, A., Bruzaud, S., Crebassa, J., Dumontet, B., Marti, E., Gorsky, G., Cozar, A., 2016. Changes in the floating plastic pollution of the Mediterranean Sea in relation to the distance to land. *PLoS One* 11, e0161581. <https://doi.org/10.1371/journal.pone.0161581>.**
- Pham, C.K., Ramirez-Llodra, E., Alt, C.H.S., Amaro, T., Bergmann, M., Canals, M., et al., 2014. Marine litter distribution and density in European seas, from the shelves to deep basins. *PLoS One* 9 (4), e95839. <https://doi.org/10.1371/journal.pone.0095839>.**
- PlasticsEurope, 2018. Plastics - the Facts 2018, an Analysis of European Plastics Production, Demand and Waste Data.
- Rabaoui, L., El Zrelli, R., Ben Mansour, M., Balti, R., Mansour, L., Tlig-Zouari, S., Guerfel, M., 2015. On the relationship between the diversity and structure of benthic macroinvertebrate communities and sediment enrichment with heavy metals in Gabes gulf Tunisia. *J. Mar. Biol. Assoc. U. K.* 95, 233–245.
- Ruiz-Orejón, L.F., Sardá, R., Ramis-Pujol, J., 2018. Now, you see me: high concentrations of floating plastic debris in the coastal waters of the Balearic Islands (Spain). *Mar. Pollut. Bull.* 133, 636–646.
- Ruiz-Orejón, L.F., Sardá, R., Ramis-Pujol, J., 2016. Floating plastic debris in the central and western Mediterranean Sea. *Mar. Environ. Res.* 120, 136–144.
- Sammari, C., Koutitonsky, V., Moussa, M., 2006. Sea level variability and tidal resonance in the Gulf of Gabès, Tunisia. *Contin. Shelf Res.* 26, 338–350.
- Schmidt, N., Thibault, D., Galgani, F., Paluselli, A., Sempéré, R., 2018. Occurrence of microplastics in surface waters of the gulf of lion (NW Mediterranean Sea). *Prog. Oceanogr.* 163, 214–220.
- Smith, W.H.F., Sandwell, D.T., 1997. Global sea floor topography from satellite altimetry and ship depth soundings. *Science* 277, 1956–1962.
- Sorgente, R., Drago, A.F., Ribotti, A., 2003. Seasonal variability in the central Mediterranean Sea circulation. *Ann. Geophys.* 21, 299–322.
- Sorgente, R., Olita, A., Oddo, P., Fazioli, L., Ribotti, A., 2011. Numerical simulation and decomposition of kinetic energy in the Central Mediterranean: insight on mesoscale circulation and energy conversion. *Ocean Sci.* 7, 503–519.
- Suaria, G., Aliani, S., 2014. Floating debris in the Mediterranean Sea. *Mar. Pollut. Bull.* 86, 494–504.
- Suaria, G., Avio, C.G., Mineo, A., Lattin, G.L., Magaldi, M.G., Belmonte, G., Moore, C.J., Regoli, F., Aliani, S., 2016. The Mediterranean Plastic Soup: synthetic polymers in Mediterranean surface waters. *Nat. Sci. Rep.* 6, 37551.
- Troupin, C., Barth, A., Sirjacobs, D., Ouberdous, M., Brankart, J.-M., Brasseur, P., Rixen, M., Alvera Azcarate, A., Belounis, M., Capet, A., Lenartz, F., Toussaint, M.-E., Beckers, J.-M., 2012. Generation of analysis and consistent error fields using the data interpolating variational analysis (diva). *Ocean Model.* 52–53, 90–101.
- Tsimplis, M.N., Proctor, R., Flather, R.A., 1995. A two-dimensional tidal model for the Mediterranean Sea. *J. Geophys. Res.* 100, C8, 16,223-16,239.
- Tunçer, S., Artüz, O.B., Demirkol, M., Artüz, M.L., 2018. First report of occurrence, distribution, and composition of microplastics in surface waters of the Sea of Marmara, Turkey. *Mar. Pollut. Bull.* 135, 283–289.
- UNEP, 2016. Marine plastic debris and microplastics – global lessons and research to inspire action and guide policy change. In: United Nations Environment Programme, Nairobi. http://www.unep.org/gpa/documents/publications/Marine_Plastic_Debris_and_Microplastic.pdf.**
- Van der Hal, N., Asaf, A., Dror, A., 2017. Exceptionally high abundances of microplastics in the oligotrophic Israeli Mediterranean coastal waters. *Mar. Pollut. Bull.* 116, 151–155.
- Veerasingam, S., Saha, M., Suneel, V., Vethamony, P., Rodrigues, A.C., Bhattacharyya, S., Naik, B.G., 2016. Characteristics, seasonal distribution and surface degradation features of microplastic pellets along the Goa coast, India. *Chemosphere* 159, 496–505.
- Wang, J., Tan, Z., Peng, J., Qiu, Q., Li, M., 2016. The behaviors of microplastics in the marine environment. *Mar. Environ. Res.* 113, 7–17.
- Wright, S.L., Thompson, R.C., Galloway, T.S., 2013. The physical impacts of microplastic on marine organisms. *Environ. Pollut.* 178, 483–492.
- Zhang, W., Zhang, S., Wang, J., Wang, Y., Mu, J., Wang, P., Lin, X., Ma, D., 2017. Microplastic pollution in the surface waters of the Bohai Sea, China. *Environ. Pollut.* 231, 541–548.